



ORIGINAL ARTICLE

Multi-parameter screening study on the static properties of nanoparticle-stabilized CO₂ foam near the CO₂ critical point



Xiakai Song^a, Xincheng Cui^a, Luming Jiang^b, Nianhao Ma^a, Yong Shu^b,
Jingzhe Li^a, Dongxing Du^{a,*}

^a Geo-Energy Research Institute, College of Electromechanical Engineering, Qingdao University of Science and Technology, Gaomi 261550, China

^b PetroChina Research Institute of Petroleum Exploration & Development, Beijing 100083, China

Received 8 October 2021; accepted 29 December 2021

Available online 4 January 2022

KEYWORDS

NP-stabilized CO₂ foam;
CO₂ critical point;
Multiple parameters;
Screen study;
Foam static properties

Abstract The important role of nanoparticles (NPs) on foam stabilization under harsh geological conditions has been well recognized. In this paper, the Orthogonal Experimental Design (OED) method is adopted to investigate the synergy effects of six parameters, including NP concentration, surfactant concentration, oil concentration, salinity, temperature, and pressure, under five levels in the range of 0–0.2 wt%, 0.1–0.5 wt%, 0–4 wt%, 0–8 wt%, 20–60 °C, and 5.5–9.5 MPa respectively. K values and B values obtained in the OED experiments are employed to show the single parameter effect and the importance of each influential factor on foam static properties. It is concluded that system temperature and pressure, which has the highest B values of 22 mm and 18 mm on foam height results, are the dominant parameters on foamability, whereas temperature with B values of 80% on foam decay rate is the dominant factor on foam stability. It is observed when the system condition is close to the CO₂ critical point, the foamability and stability of the NP-stabilized foam are much worse than under conditions far from the critical point. At last, optimal formulation of surfactant and NP concentration is proposed and validated for two geological cases of 45 °C and 55 °C with salinity and oil presence. It is expected the experimental technique, as well as the research results, reported in this paper could help the laboratory screening and formulation optimization of the complex NP-stabilized ScCO₂ foam system.

© 2022 The Author(s). Published by Elsevier B.V. on behalf of King Saud University. This is an open access article under the CC BY license (<http://creativecommons.org/licenses/by/4.0/>).

* Corresponding author.

E-mail address: du-dongxing@qust.edu.cn (D. Du).

Peer review under responsibility of King Saud University.



1. Introduction

Nowadays, the emission of CO₂ into the atmosphere has increased dramatically (Gil-Alana and Monge, 2020), and the resulting greenhouse effect has shown serious negative impacts on human lives (Li et al., 2019; Tom-Dery et al., 2018; Beach et al., 2019). CO₂ Enhanced Oil Recovery (CO₂-EOR), which contributes as one of the most efficient

techniques in the Carbon Capture, Utilization, and Storage (CCUS) chain, has attracted worldwide research interests (Jun et al., 2013; Akinnikawe et al., 2010; Song et al., 2020). Due to the low viscosity of gas-phase CO₂, gas channeling often occurs when CO₂ gas displacement is performed in the field of heterogeneous reservoir oilfields (Majeed et al., 2021). Therefore, the application of CO₂ foam is a common method to improve maneuverability control in carbon dioxide floods. At present, the use of foam flooding has become a popular enhanced oil recovery (EOR) method used in non-uniform reservoirs and fluidity control in uniform reservoirs (Li et al., 2012; Al Sumaiti et al., 2017; Guo and Aryana, 2016).

The higher viscosity but lower density of foam allow this displacement technology to give better recovery factors by improving the areal and vertical sweep, reducing viscous fingering, and providing better recovery factors by diverting gas from high permeable zones (Pang et al., 2018; Yu et al., 2012). In addition, foam can block high-permeability reservoirs and increase the volume of the flood during oil displacement. The presence of crude oil can destroy the foam structure and rupture it, making the foam have the ability to “plug water and not oil” advantage. Therefore, by injecting CO₂ foam into the reservoir for oil extraction, the gas flow can be effectively controlled, and the volume sweep efficiency in the process of displacing oil can be expanded to increase the oil extraction rate. This technology has been widely used in oil field operations in many countries for many years (Majeed et al., 2021; Pang et al., 2018; Chen et al., 2014; Skauge et al., 2002; Du et al., 2021; Fernø Martin et al., 2016).

However, limited by the chemical properties of the foaming agent and external conditions, the stability of ScCO₂ foam in practical applications is usually not robust and is easy to defoam after being exposed to crude oil and to decompose under high salinity, high-pressure, and high-temperature reservoir conditions (Osei-Bonsu et al., 2015; Wang et al., 2017; Aarra et al., 2014).

With the development of nanotechnology in recent years, a variety of preparation processes have been developed to produce NPs that can meet the manufacturing needs of various industries (Jun et al., 2013; Shokouhimehr et al., 2018; Hosseini-Nasab et al., 2016; Ahadi et al., 2019; Kim et al., 2015). It was found that adding NPs to the surfactant solution can effectively increase the stability of ScCO₂ foam (Ko and Huh, 2019; Dehdari et al., 2020; Singh and Mohanty, 2020; AlYousef et al., 2017). In an NP-stabilized foam, the NPs adsorbed on the gas-liquid interface will form a liquid film with higher mechanical strength, which can effectively reduce the discharge rate, prevent the liquid film from being disturbed and broken, and thereby enhance the foam stability. In addition, the NPs and surfactant molecular adsorbed in the gas-liquid interface can form a spatial network structure, which can increase the thickness of the liquid film and act as a barrier to liquid discharge and gas diffusion, thus preventing liquid film rupture and bubble coarsening (Fan et al., 2020; Farhadi et al., 2016; Prigiobbe et al., 2016).

As a complex system, the NP-stabilized foam system involves many influential factors, such as NP hydrophilicity and hydrophobicity, NP size, NP type, surfactant type, NP concentration, surfactant concentration, system pressure, temperature, oil presence, salinity, and so on, which make it a fascinating research topic to the worldwide scholars. For instance, Yu et al. (2014) investigated the effect of particle hydrophobicity on CO₂ foam generation and observed more CO₂ foam generated as the particle surface changed from hydrophilic to hydrophobic. Li et al. (2017) investigated the effects of hydrophilic SiO₂ NPs and cetyltrimethylammonium bromide (CTAB) on the stability of CO₂ foam and found the half-life of CTAB/SiO₂-stabilized CO₂ foam increased at the higher NP concentration. AlYousef et al. (2017) found the half-life of N₂ foam stabilized by SiO₂ NPs is 5 to 8 times higher than that of using surfactant alone. Emrani and Nasr-El-Din (2015) found that the optimal concentration of SiO₂ NPs is 0.1 wt%, and the half-life of the SiO₂/AOS (α -olefin sulfonate)

foaming solution is about one hour longer than that of the AOS solution. Bashir et al. (2019) found that adding 0.2 wt% SiO₂ NPs at 85 °C had the best effect on increasing the stability of CO₂ foam under oil presence and salinity conditions. Emrani et al. (2017) found the addition of NPs will promote the formation of fine foam, thereby increasing the apparent viscosity of the foam and improving the stability of CO₂ foam at high-temperature and high salinity conditions. (Wang et al., 2017) studied the influences of temperature, pressure, salinity on CO₂ foaming capability and they found the performance of CO₂ foams at high-temperature and pressure is greatly dependent on the hydrophilic-lipophilic balance (HLB) value of surfactants. They recommended combined or mixed surfactants for the generation of the CO₂ foams with good performance at high-temperature conditions. (Harati et al., 2020) assessed various hydrophilic NP types and concentrations on the stability of CO₂ foams and discovered the optimum NP concentration of 0.008 wt% for producing CO₂ foams. (San et al., 2017) reported increased foamability and stability and decreased mobility of NP-stabilized CO₂ foam with the increasing NaCl concentration from 1.0 wt% to 10 wt%.

Based on the above literature analysis, it is found most researchers focus on limited parameters in their studies with the controlled variable method, that is, study the influence of a factor through changing the level of this factor while keeping other factors constant. Although the controlled variable method can obtain accurate and clear results, it may take too many experimental rounds for multiple parameter studies and therefore is only effective for small-scale, few-factor experimental designs. As a complex system with synergistic multiple parameters, the challenging multi-factor multi-level screening studies, as well as the optimal formulation determination of the NP-stabilized CO₂ foam under geological conditions, are scarcely reported so far.

As an effective experimental design technique, the orthogonal experimental design (OED) has been applied in many industrial fields on studying the effects of multiple factors effects as well as screening the optimal factor combinations (Deng et al., 2018; Li, 2020; Wang et al., 2020; Zhu et al., 2013). Employing the Taguchi parameter design methodology (Antony, 2006), the OED arranges the multiple parameter experimental studies in a much smaller number of runs as compared to the controlled variable method. In a very recent study, (Du et al., 2020a) employed the OED method on parameter screening study for optimizing the static properties of NP-stabilized CO₂ foam. They considered five influential factors of NP size, surfactant concentration, NP concentration, temperature, and salinity at four different levels of 7–40 nm, 0–0.15 wt%, 0–0.2 wt%, 25–55 °C, and 0 – 3 wt%, respectively. Based on the obtained optimal formulations on foam static properties, (Du et al., 2020b) generated the NP-stabilized foam with satisfactory rheological properties. It has to be mentioned, however, the multiple parameter research performed by (Du et al., 2020a) was under the atmospheric environment which left the important parameter of pressure (Vishal, 2017; Zhang et al., 2008) out of consideration.

In this paper, therefore, the OED method is used to study the comprehensive influence of the six key factors, including surfactant concentration, NP concentration, oil concentration, salinity, system pressure, and temperature, on the static properties of NP-stabilized CO₂ foam. Based on the well-recognized facts that the smaller size NPs could generate more stable foams (Deng et al., 2018) and the combination of hydrophilic NPs with surfactant is more widely employed than the pure hydrophobic NPs (Dehdari et al., 2020; Harati et al., 2020; Rezvani, 2020; Yekeen, 2018), we didn't take NP size and NP hydrophobicity into consideration in this paper. The screening investigations, therefore, are carried out based on six-factor five-level OED schemes. We studied the effect of each factor as well as determined the dominant factors on foam static performances, and validated our research by proposing an optimal formulation to produce NP-stabilized ScCO₂ foam with satisfactory foamability and foam stability results under given geological conditions.

2. Experimental

2.1. Materials and devices

In the experiment, CO₂ with a purity of 99.9% is used as the foam internal phase and AOS is employed as the surfactant. The solution salinity is controlled by dissolving different masses of NaCl (analytical purity, provided by Tianjin Bodi Chemical Co., Ltd.) and the oil presence is simulated by adding kerosene to the solution. The SiO₂ NP (NP300 provided by the German Evonik company) with average particle size of 7 nm, specific surface area of $300 \pm 30 \text{ m}^2/\text{g}$ and purity higher than 99.8%, is employed in this study. XRD test (Beijing Jiade Lida Technology Co., Ltd., Miniflex 600) has been performed to validate the SiO₂ concentration in the NP. As shown in Fig. 1, only one peak is observed at diffraction degree of 22 corresponding to SiO₂, which validates the high material purity.

2.2. Experimental setup

Fig. 2 shows the schematic diagram of the experimental setup (model TCXPH-25, Jiangsu Tuochuang Technology Instrument Co., Ltd.), which mainly consists of the CO₂ pressurization system and the H-T and H-P CO₂ foam generation system. In the CO₂ pressurization system, the CO₂ gas from the cylinder was pressurized through the piston pump until it approaches the designated pressure. Then the pressurized CO₂ was injected into the H-T and H-P system whose control pressure range up to 15 MPa and the control temperature range up to 80 °C, in which the CO₂ is heated to the designated temperature and is kept for a period to achieve the stable condition with the pre-injected NP-surfactant solution. Foam is then generated through the magnetic stirring system with rotating speed up to 1350r/min and the foam height as well as the defoaming time is monitored to characterize the static properties of the NP-stabilized CO₂ foam at H-T and H-P conditions.

Fig. 3 shows H-T and H-P observation vessel, which is the key part of the experimental setup, together with the picture of the generated NP-stabilized foam column inside the vessel. The foam height, as well as the foam height variation situation,

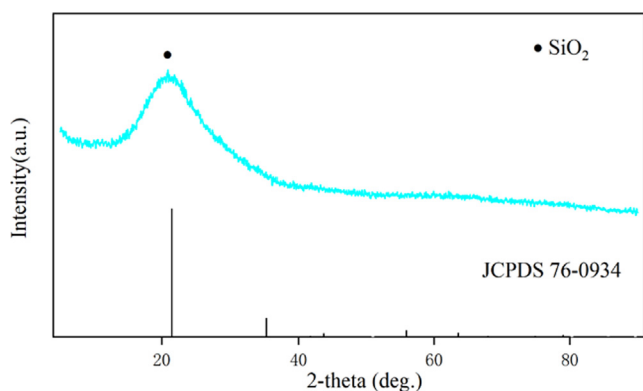


Fig. 1 XRD test result on NP with comparison of PDF#76-0934 card of standard SiO₂.

could be clearly observed and recorded for foam static behavior analysis.

2.3. Preparation of NP-surfactant mixture solution

Fig. 4 shows the preparation process of the NP-surfactant solution. Firstly, a certain mass of NPs, surfactants, kerosene, and salt are mixed into 100 ml deionized water in an Erlenmeyer flask. Secondly, the mixture solution is agitated with a magnetic stirrer (model 79-1, Changzhou Huapuda Teaching Instrument Co., Ltd.) at a speed of 1200 rpm for continuous 2 h. Thirdly, the mixture solution is transferred to the ultrasonic disperser (model YL-060ST, Shenzhen Yulu Cleaning Equipment Co., Ltd.) at a frequency of 40kHz for 2 h under a controlled temperature to avoid surfactant degradation. At last, the dispersion solution is kept rest under room condition for 24 h to check the solute stability in the mixture. As shown in Fig. 4(d), the NP dispersion does not show macroscopic aggregation during the holding period, which indicates the prepared NP-surfactant solution is suitable for foam generation practices. It is demonstrated that satisfactory NP solution could be prepared with this process (Du et al., 2020a).

2.4. Generation of the NP-stabilized CO₂ foam

As shown in Fig. 5, the detailed steps for generation of the NP-stabilized CO₂ in the H-T and H-P vessel are described in the sequence of Fig. 5 (a)-(d) as follows,

- Inject CO₂ gas to the vessel under the experimental temperature and keep it flowing for 1 min to exhaust the air inside the vessel;
- Inject 20 ml of NP-surfactant solution, then inject high-pressure CO₂ into the vessel until the pressure inside the vessel reaches the designated level. Remain in the system for a certain period until the system pressure and temperature becomes stable.
- Agitate the solution inside the vessel with the magnetic stirring system at 1350 rpm for a certain period (10 min in this study), and record the foam height at the end of the stirring to characterize the foaming ability of the NP-surfactant solution.
- After the stirring stops, let the generated foam rest in the vessel for a certain period (30 min in this study), and record the foam height decrease with time to characterize the decay behavior of the NP-stabilized CO₂ foam.

2.5. Evaluation criteria on foam static properties

The evaluation indicators of the static properties of the bulk foam are usually foam height (or foam volume) and foam half-life (AlYousef et al., 2017; Fan et al., 2020; Farhadi et al., 2016), which are employed to the characterization of the two aspects of foaming ability (foamability) and foam stability respectively. The foam height is obtained after the surfactant solution undergoes a sufficient foaming process, and the higher foam height indicates the better foaming ability of the surfactant solution. The foam half-life is the time taken for the generated foam column to decay to half of the original

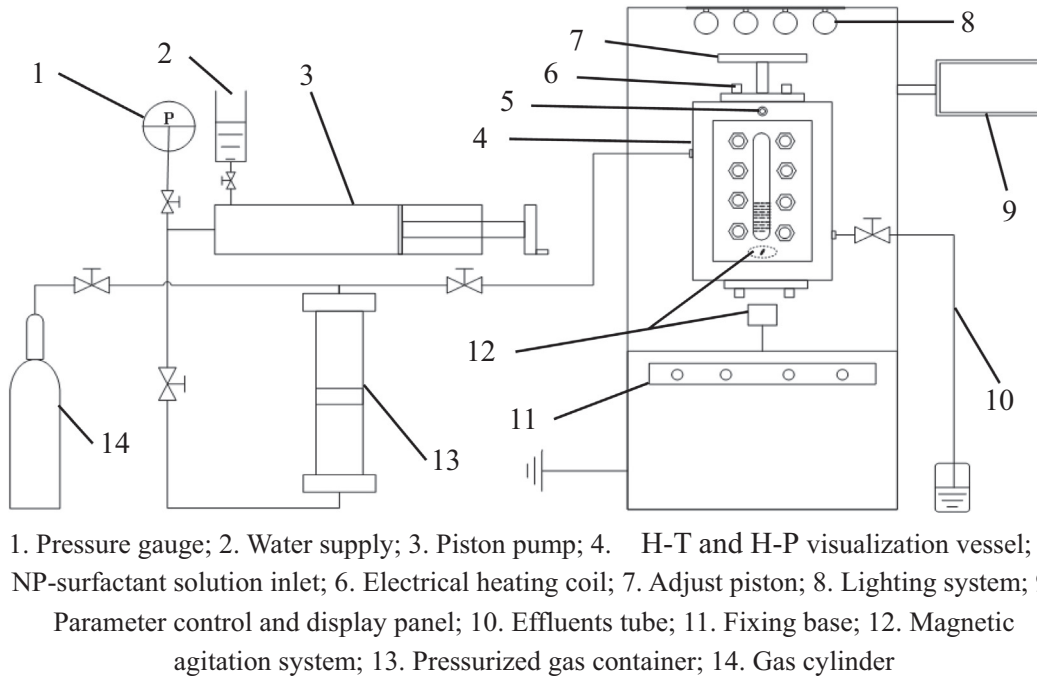


Fig. 2 Schematic diagram of the H-T and H-P foam characterization system. 1. Pressure gauge; 2. Water supply; 3. Piston pump; 4. H-T and H-P visualization vessel; 5. NP-surfactant solution inlet; 6. Electrical heating coil; 7. Adjust piston; 8. Lighting system; 9. Parameter control and display panel; 10. Effluents tube; 11. Fixing base; 12. Magnetic agitation system; 13. Pressurized gas container; 14. Gas cylinder.

height, and the longer foam half-life indicates better foam stability.

In this study, we employ the foam height value after 10 min' agitation process $E_{fg,10min}$ as the indicator for foamability, and evaluate the foam stability with the foam decay rate after 30 min' resting period $E_{fd,30min}$, as defined in Eq. (1),

$$E_{fd,30min} = \frac{h_1 - h_2}{h_1} \quad (1)$$

where h_1 is the foam height after agitation, and h_2 is the foam height after 30 min resting time in the H-T and H-P vessel. Higher $E_{fd,30min}$ value reflects larger foam height reduction and thereby indicates lower foam stability.

The two indicators are employed based on the observations on the typical foam generation and foam decay behavior in the experiments. Fig. 6 (a) shows the typical foam height variation history in the foam generation process, indicating the foam height remains nearly constant after 10 min agitation process. Therefore $E_{fg,10min}$ is taken as the proper measure of foamability. The foam decay behavior is shown in Fig. 6 (b), on the other hand, indicates the foam decay process may finish within 30 min after the agitation process without reducing to the half value of the original height at all even after 5 h resting period. It is believed the foam height decrease within 30 min could reflect reasonably the foam stability behavior, therefore the parameter of $E_{fd,30min}$ instead of half-life is employed in this study to evaluate the property of foam stability.

2.6. Experimental scheme based on OED method

OED method is employed to design the experimental scheme for studying the static properties of the complex

NP-stabilized ScCO_2 foam system. As shown in Table 1, six influential factors, including surfactant concentration, NP concentration, oil concentration, salinity, pressure, and temperature, are taken into consideration and each factor is studied in five levels in the range of 0.1–0.5 wt%, 0–0.2 wt%, 0–4 wt%, 0–8 wt%, 5.5–9.5Mpa, and 20–60 °C respectively.

The level values for various influential factors are set based on literature reported works. Five levels of 0, 0.05, 0.1, 0.15 and 0.2 wt% have been adopted for the factor of surfactants concentration (Singh and Mohanty, 2015, 2020); and five levels of 0, 0.05, 0.1, 0.15 and 0.2 wt% are set for the second factor of NP concentration (Rognmo et al., 2017; Emrani and Nasr-El-

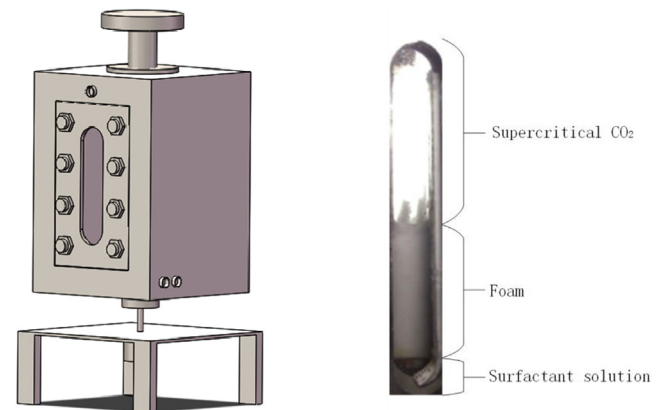


Fig. 3 H-T and H-P vessel with the generated NP-stabilized CO_2 foam. (a) Weighing of solute materials; (b) 2-hours magnetic stirring; (c) 2-hours ultrasonic dispersing; (d) 24-hours resting test.

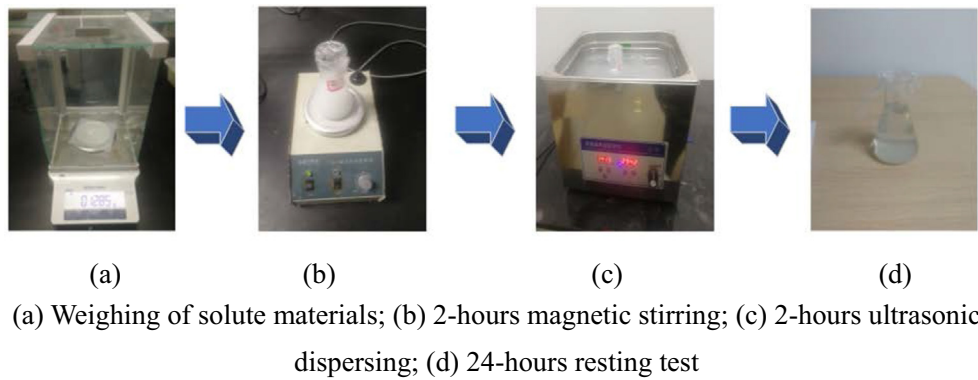


Fig. 4 The preparation process of the NP-surfactant mixture solution.

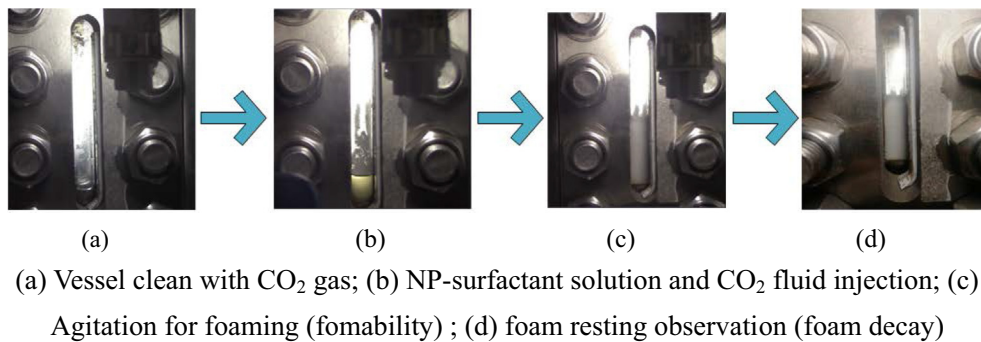


Fig. 5 Detailed steps on NP-stabilized CO₂ foam generation and rest process.

Din, 2017; Fu and Liu, 2020). The factor of temperature, which has a profound impact on the stability of the foam (Fan, 2020; Fu and Liu, 2020), are selected at five levels of 20, 30, 40, 50 and 60 °C based on the typical geological conditions as well as the critical point of CO₂. Pressure is one of the most influential factor for NP-stabilized foam static characteristics (Wang, 2017; Zhang, 2019); and was set in this study at five typical geological levels of 5.5, 6.5, 7.5, 8.5 and 9.5 MPa, which covers the critical pressure point of CO₂ of 7.29 MPa

as well. Oil is generally considered to be harmful to foam, and the five oil concentration levels are set at 0, 1, 2, 3 and 4 wt% (Pang et al., 2018; Telmadarreie and Trivedi, 2020; Yang et al., 2017b; Zhao and Torabi, 2020). As NaCl component usually dominating the saline composition, (Eftekhari et al., 2015; San et al., 2017; Yang, 2017a) we employ the NaCl solution as the representative saline and take five salinity values of 0, 2, 4, 6 and 8 wt% in the OED table to focus on the influential factor of salinity.

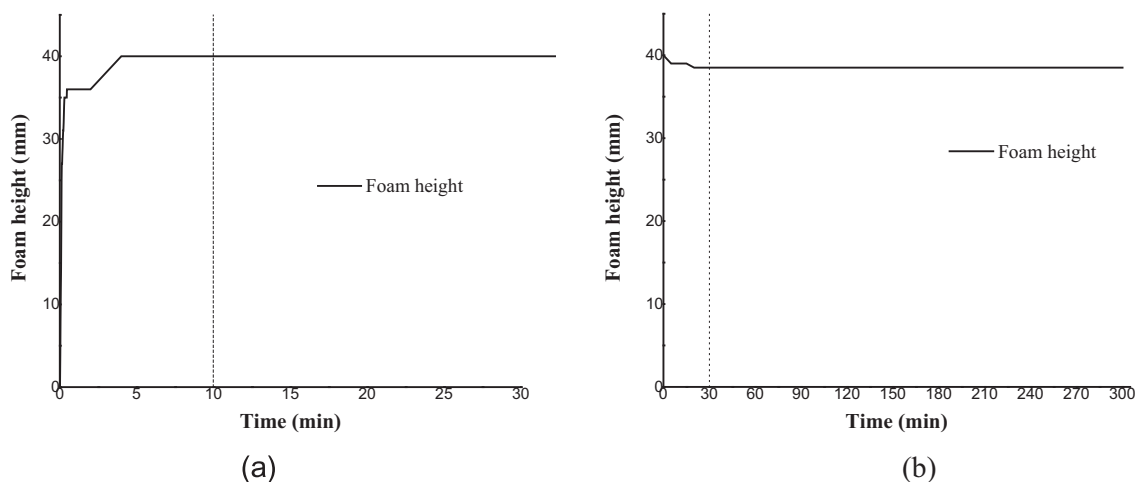


Fig. 6 Typical results on foam height variation with time in: (a) foam generation process; and (b) foam rest stage.

Table 1 The complex system with six influential factors under five levels.

	Surfactant concentration	NP concentration	Oil concentration	Salinity	Pressure	Temperature
	wt%	wt%	wt%	wt%	MPa	°C
1	0.1	0	0	0	5.5	20
2	0.2	0.05	1	2	6.5	30
3	0.3	0.1	2	4	7.5	40
4	0.4	0.15	3	6	8.5	50
5	0.5	0.2	4	8	9.5	60

Under the OED scheme, the number of experimental groups involving six factors at five levels can be confined to 25 groups based on the standard orthogonal table, which is much less than the experimental scheme supplied with the controlled variable method, thereby significantly reducing the workload. The detailed parameter combinations for the 25 experiments based on the OED method are listed in Table 2.

In the OED method, the effect of each influential factor can be evaluated through parameter K based on the mean level value analysis, and the significance of each factor on the foam static properties can be analyzed with parameter B based on the range analysis of the obtained K values. In the experimental scheme with five levels for each factor, the mathematical formula for calculating K and B values are given in Eq. (2) and Eq. (3) as follows,

$$K_i = \frac{S_i}{s} \quad (i = 1, 2, 3, 4, 5) \quad (2)$$

$$B = \max\{K_1, K_2, K_3, K_4, K_5\} - \min\{K_1, K_2, K_3, K_4, K_5\} \quad (3)$$

where S_i represents the sum of the experimental results corresponding to the i -th level, and s represents the number of levels corresponding to the factor in the orthogonal table. While B value is the difference between the maximum K value and the minimum K value for a certain factor.

3. Results and discussion

3.1. Summary of experimental results on foam static properties

Table 2 summarize the detailed experimental conditions as well as the obtained foam height and foam decay rate results of all the 25 OED experiments.

Fig. 6 and Fig. 7 shows, in summary, the measured foam heights and the foam decay rates for all the 25 experiments as listed in Table 2.

As shown in Fig. 7 (a), the foam height obtained under different compositions varies remarkably from negligible small (group 1, 14) to 40 mm (group 5, 8). Whereas the results in

Table 2 Experimental scheme for the six-factor five-level system with OED.

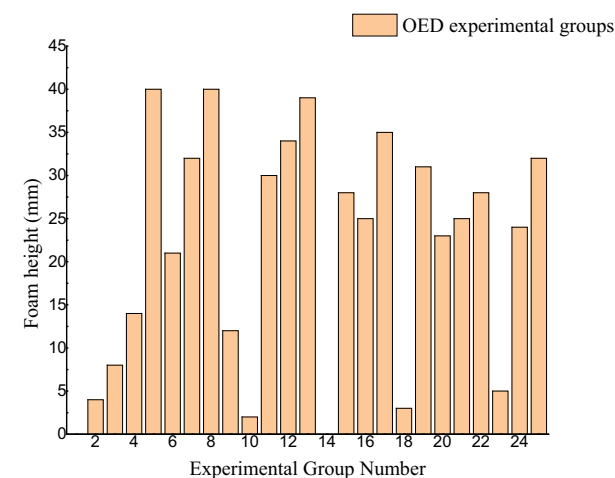
Test no.	Surfactant concentration	NP concentration	Temperature	Pressure	Oil concentration	Salinity	Height	Decay rate
	wt%	wt%	°C	MPa	wt%	wt%	mm	*100%
1	0.1	0	30	5.5	0	0	0	1
2	0.1	0.05	40	6.5	1	2	4	1
3	0.1	0.1	50	7.5	2	4	8	0.25
4	0.1	0.15	60	8.5	3	6	14	0.2
5	0.1	0.2	20	9.5	4	8	40	0.08
6	0.2	0	40	7.5	3	8	21	0.76
7	0.2	0.05	50	8.5	4	0	32	0.37
8	0.2	0.1	60	9.5	0	2	40	0.03
9	0.2	0.15	20	5.5	1	4	12	0.2
10	0.2	0.2	30	6.5	2	6	2	1
11	0.3	0	50	9.5	1	6	30	0.66
12	0.3	0.05	60	5.5	2	8	34	0.24
13	0.3	0.1	20	6.5	3	0	39	0.09
14	0.3	0.15	30	7.5	4	2	0	1
15	0.3	0.2	40	8.5	0	4	28	0.03
16	0.4	0	60	6.5	4	4	25	0.64
17	0.4	0.05	20	7.5	0	6	35	0.17
18	0.4	0.1	30	8.5	1	8	3	1
19	0.4	0.15	40	9.5	2	0	31	0.04
20	0.4	0.2	50	5.5	3	4	23	0.13
21	0.5	0	20	8.5	2	2	25	0.2
22	0.5	0.05	30	9.5	3	4	28	0.75
23	0.5	0.1	40	5.5	4	6	5	0.32
24	0.5	0.15	50	6.5	0	8	24	0.17
25	0.5	0.2	60	7.5	1	0	32	0.17

Fig. 7(b) indicate the foam could show either the best stability behavior with the negligible small decay rate of 0.032 at group 15, or the worst behavior with a decay rate of 1 for groups 1, 2, 10, 14, and 18. The results in both figures show the synergistic effect of the studied factors on the foam static properties, and therefore necessitate the in-depth screening studies of the multiple parameter complex system.

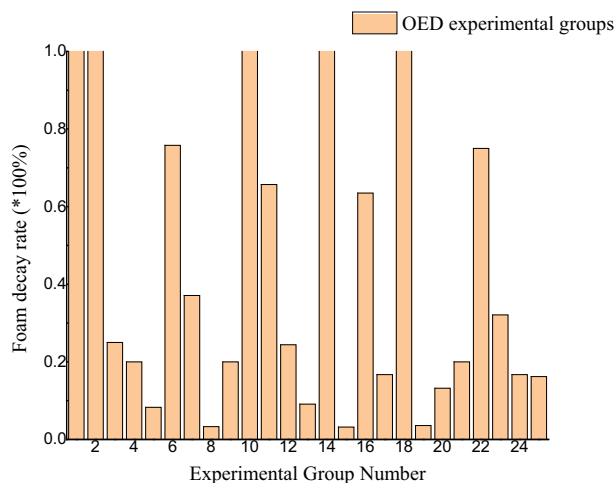
3.2. Effects of single parameter on foam static properties

3.2.1. Surfactant concentration

Fig. 8 shows simultaneously the effect of surfactant concentration on the static properties in terms of foam height and foam decay rate. It is observed that with the increasing surfactant concentration from 0.1 wt%~0.3 wt%, the foam height rises from 12 mm to 26.2 mm. Thereafter the foam height remains nearly constant, which indicates a surfactant concentration over 0.3 wt% could be proper for NP-stabilized foam generation. The foam decay rate results, as displayed as red triangle line and marked in the right Y-axis, show the unanimous



(a)



(b)

Fig. 7 Summary of the (a) Foam height and (b) foam decay rate results for all the 25 OED designed experiments.

decreasing trend from 0.5 to 0.32 with the increasing surfactant concentration from 0.1 wt%~0.5 wt%, indicating the higher surfactant concentration would benefit the foam stability behavior as well.

According to Prigiobbe et al., 2016 the higher concentration of surfactant could enhance the mechanical strength of the foam film, which makes the liquid film and the plateau boundary layer immobile and thereby prevents the occurrence of convective NP transport. Another reason for the long life of the liquid film with higher surfactant concentration could attribute to the in-situ surface activation of NPs to moderate hydrophobicity, which results in a high tendency of the NPs to adsorb strongly at the gas-liquid interface to make the bubble less prone to rupture and maintain stability within a specified time

3.2.2. NP concentration

Fig. 9 shows the influence of the concentration of SiO₂ NPs on the foam static properties based on the K values of the foam height and the foam decay rate results.

It is found the NP concentration didn't show a significant effect on the foam generation, with the foam height fluctuating within 16.2–26.6 mm in the NP concentration range of 0 ~ 0.2 wt%. On the other hand, the effect of NP concentration on the foam stability improvement is quite obvious. With the increasing NP concentration from 0 ~ 0.1 wt%, a sharp decrease of foam decay rate from 0.65 to 0.32 is observed, indicating the significant effect of NP presence on foam stability enhancement. With the further increase of NP concentration above 0.1 wt%, its influence on foam stability improvement is still obvious however with a gentler slope to reach the minimum value of 0.282 at the concentration of 0.2 wt%.

The reason behind the observation that higher NP concentration leads to higher foam stability could attribute to the synergistic effect of NPs and surfactant. As referred to Prigiobbe et al. (2016); an extra amount of NPs could adhere to the surface of surfactant particles (since the molecules of NPs are much smaller than surfactants), or fill between larger surfactant particles, to further enhance the mechanical strength of the foam liquid film and reduce the foam annihilation caused by gravity drainage (Alwated and El-Amin, 2021; Bashir

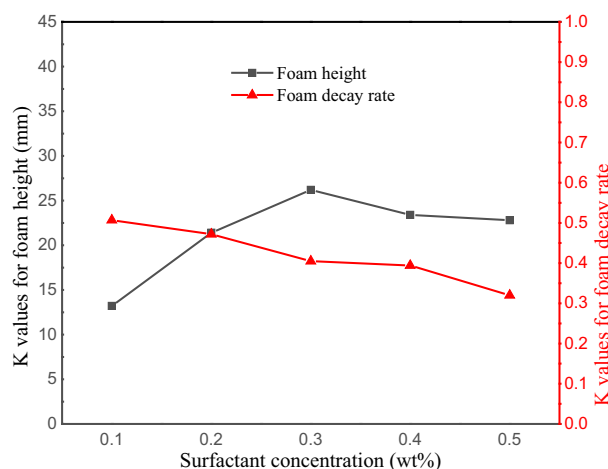


Fig. 8 Effect of surfactant concentration on the foam static properties.

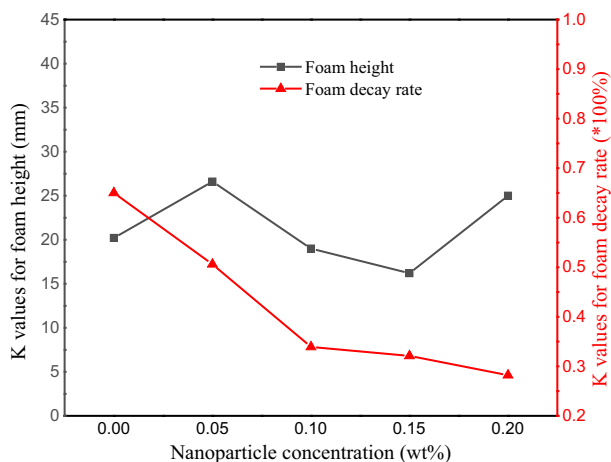


Fig. 9 Effect of the NP concentration on the foam static properties.

et al., 2019). While after reaching a certain concentration (critical) value, more NPs remaining in the surfactant solution could not contribute further to stability enhancement, and thereby become “ineffective NPs”. The critical NP concentration, as revealed in Fig. 9, is 0.1 wt%.

3.2.3. Oil concentration

Fig. 10 shows the effect of oil presence on the foam static properties based on the foam height and foam decay rate results in the oil concentration range 0 ~ 4%.

It is observed from the figure that the oil existence doesn't show the significant influence of foamability in the studied concentration range, with the generated foam height varying between 16.2 and 25.4 mm. While the slightly negative effect of oil existence on foam stability could be deduced from the figure based on the general upward-directed red line reflecting the relationship between the foam decay rate and the increasing oil concentration. The most stable foam is obtained at the situation without oil existence with a foam decay rate of 0.28, whereas the foam stability slightly decreased with the foam decay rates of 0.35–0.6 at a higher oil concentration range of 0.1 wt-0.5 wt%. Although the oil presence could

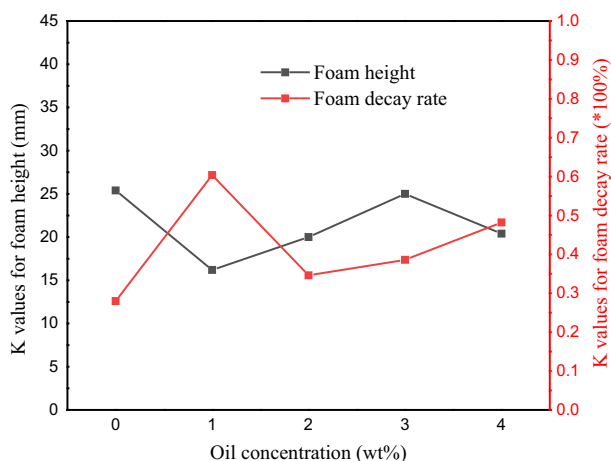


Fig. 10 Effect of oil concentration on the foam static properties.

reduce the foam stability, the foam decay rate for NP-stabilized foam could still maintain in an acceptable range after 10 min's resting time.

It is generally believed that the presence of oil is very destructive on foam and the destabilizing effect of light oils (such as kerosene employed in this study) on foams is more serious than heavy oils (Deng et al., 2018). It is found from Fig. 10, however, the oil concentration effect is alleviated due to the adding of NPs, which could be attributed reasonably to the ability to prevent oil spread at the liquid film due to the adsorption and aggregation of NPs at the foam lamellae (Deng et al., 2018).

3.2.4. Salinity

Fig. 11 shows the effect of solution salinity on the foam height and foam decay rate results in the range of 0 ~ 8 wt%. It could be deduced that in the NP-stabilized foam, the effect of surfactant solution salinity on both foam static properties is not significant. In the given salinity range, the K values of the foam height fluctuate between 17.2 mm and 26.8 mm, and the foam decay rate varies in the range of 0.33 to 0.56 without showing clear dependency on the salinity.

Although the presence of salt could influence significantly on the static properties of surfactant foam, the salinity has little effect on the foamability and stability of the NP-stabilized foam. According to the Derjaguar -Landau-Verwey-Overbeek (DLVO) theory, NP-stabilized foam is simultaneously subjected to electrostatic repulsion and van der Waals force (Maestro et al., 2014). Especially in these study cases, it is likely that the existence of NaCl could increase the hydrophobicity of the non-polar molecular SiO_2 due to their presence as anion-cationic pair in the aqueous dispersion (Xiao et al., 2017).

3.2.5. Pressure

Fig. 12 shows the K values of the foam height and the foam decay rate at the system pressure of 5.5 MPa, 6.5 MPa, 7.5 MPa, 8.5 MPa, and 9.5 MPa respectively. It is observed the foamability gradually increases in the pressure range 5.5 MPa-8.5 MPa, while it rises sharply after 8.5 MPa and finally reaches the highest foam height of 33.8 mm. The experimental observations are consistent with those reported by Yu

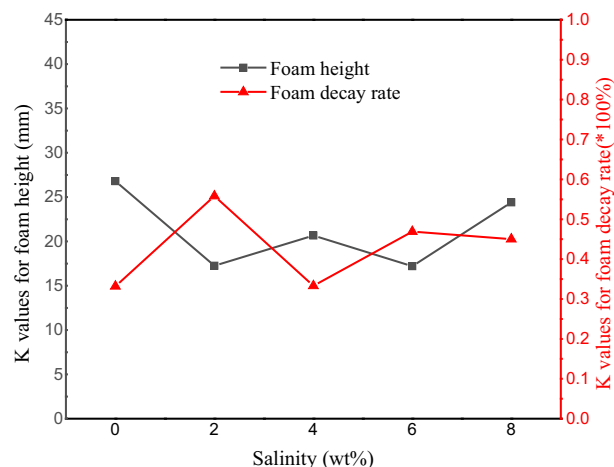


Fig. 11 Effect of salinity on the foam static properties.

et al. (2012) and the reason behind this phenomenon may be contributed to the decreased interfacial tension between CO₂ and brine at higher pressure conditions, and the lower gas–water interfacial tension promotes the foam formation process.

On the other hand, it is found the foam stability shows the worst behavior at 6.5 MPa, where the K values for foam decay rate have the highest values of 0.58. The foam decay rates decrease gradually with the increasing pressure after 6.5 MPa and reach the minimum value of 0.312 at 9.5 MPa. The enhanced stability at higher system pressure may be attributed to the increased ScCO₂ density and cohesive energy density (Dhanuka et al., 2006), which could enhance the interaction between the CO₂ phase and the surfactant molecules to firmly attach the NPs to the liquid film and the Plateau border (Zhang et al., 2015).

3.2.6. Temperature

Fig. 13 shows the influence of the temperature on the K values of the foam height and the foam decay rate in the range 20 °C ~ 60 °C. The worst foamability with the lowest foam height of 6.6 mm and the worst foam stability with the highest foam decay rate of 0.95 is obtained at 30 °C, which is quite close to the CO₂ supercritical temperature of 31.1 °C. The NP-stabilized foam static performance under other studied temperatures, on the other hand, behaves satisfactorily with the K values of foam height and the foam decay rate located in the range of 17.8 ~ 30.2 mm and 0.15 ~ 0.43 respectively. It is deduced, therefore, the phase transition of the internal phase of CO₂ may affect significantly the foam static behavior.

3.3. Range analysis of various influential factors

After obtaining the effect of every single parameter on foam static properties, range analysis based on the B values as described in Eq. (3) is performed to distinguish the significance of each factor on the foam generation capacity and the stability of the NP-stabilized CO₂ foam.

Fig. 14 and Fig. 15 display the B values of the studied six factors, including surfactant concentration, NP concentration, temperature, pressure, oil concentration, and salinity, on the foam height and foam decay rate results respectively. As

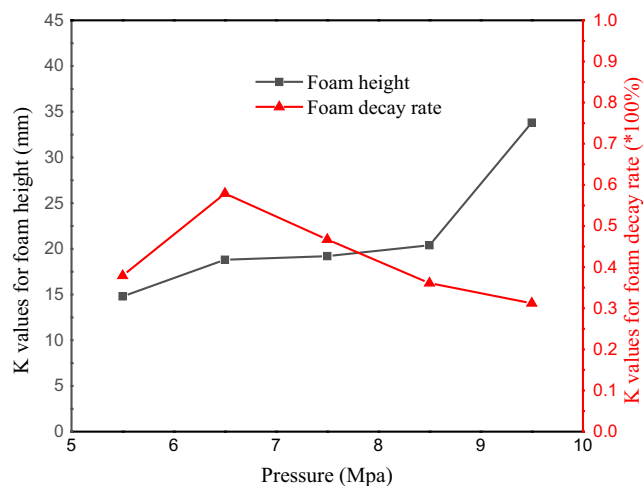


Fig. 12 Effect of pressure on the foam static properties.

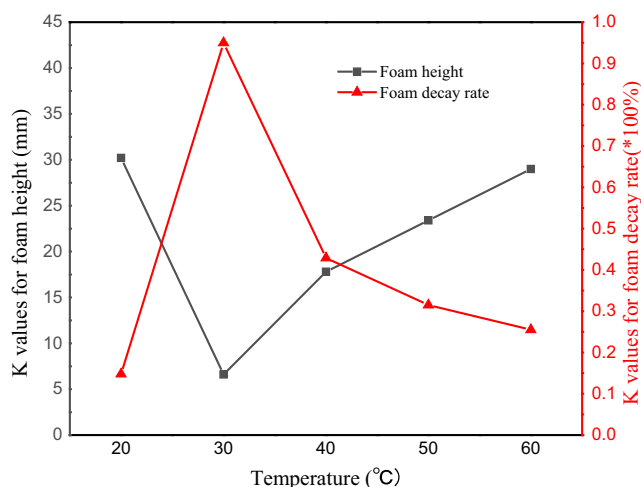


Fig. 13 Effect of temperature on the foam static properties.

shown in Fig. 14, the factor which affects most remarkably foam generation is temperature, followed by pressure, surfactant concentration, NP concentration, salinity, and oil existence in significance based on the decreasing B values. It is also observed from the figure that the influence of temperature and pressure on foamability is more obvious than the other four factors. As shown in Fig. 15, on the other hand, the dominant factor for foam stability is temperature, followed by NP concentration, oil concentration, pressure, salinity, and surfactant concentration.

Based on the range analysis results, the synergy effect of various factors on foamability and foam stability could be observed. It is concluded that an NP-stabilized foam with satisfactory static behaviors may not be obtained through solely adding as high concentration as possible of NPs and surfactants, the geological conditions, such as temperature, pressure, oil existence, and salinity, should also be taken into consideration for foam formulation determinations for its successful field applications.

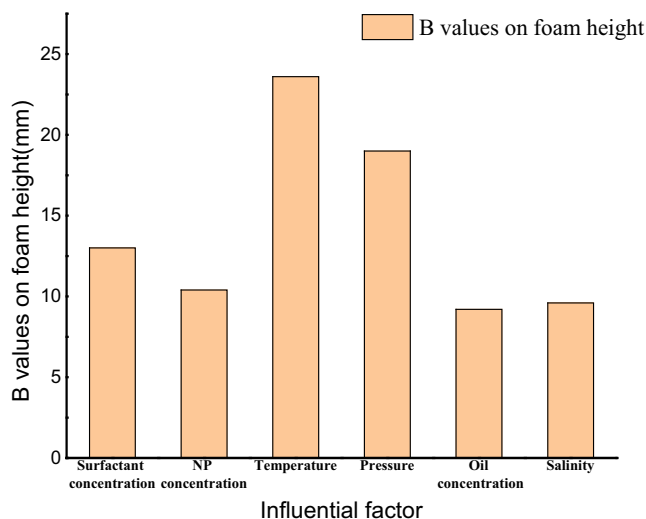


Fig. 14 Range analysis of various influential factors on the foam height results.

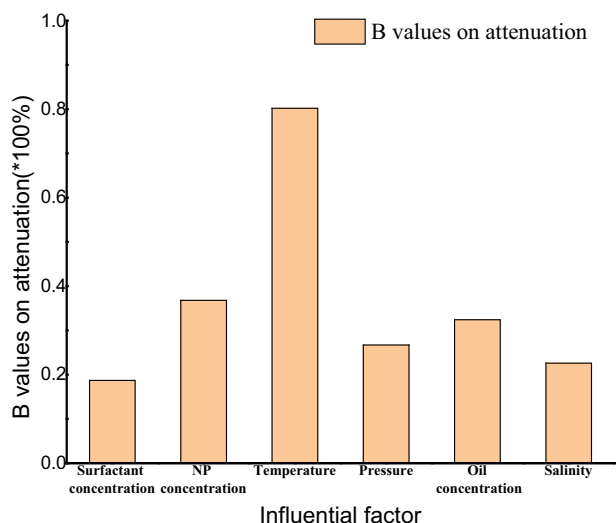


Fig. 15 Range analysis of various influential factors on the foam decay rate results.

3.4. Synergy effects of pressure and temperature on foam static properties

The temperature and pressure were the most significant factors for the foam generation capacity, while the temperature is the most significant factors for the foam stability behavior. To reveal the synergy effect of the two parameters, temperature and pressure, Figs. 16 and 17 display the foam height and foam decay rate results for all the 25 sets of experiments in 3D diagrams with the two independent variables of temperature and pressure in the X-axis and Y-axis.

It is observed from Fig. 16 that the foam generation capacity has poor behavior in the pressure range of 5.5 ~ 7.5 MPa at 30 °C, which is quite close to the critical points of CO₂. At 30 °C and 7.5MPa, no foam column is generated at all. Under conditions far from the critical points, on the other hand, the NP surfactant mixture gives satisfactory foamability results. The foam decay rates results, as displayed in Fig. 17, also indicate the worst foam stability behavior around the CO₂ critical pressure and temperature condition. The foam decay rate shows the highest value of 1.0 in the pressure range 5.5 ~ 8.5 MPa at 30 °C, and a pressure of 6.5 MPa at 40 °C. Whereas under conditions far from the critical points, the stability of the NP-stabilized foam behaves well.

It is concluded, therefore, the synergy effect of temperature and pressure relates tightly with the phase behavior of the internal CO₂ phase. When operating near the phase transition point of CO₂, it could be a challenge to obtain an NP-stabilized foam with satisfactory static properties.

3.5. Foam formulation optimization under geological conditions

Based on the above analysis of the influence of various factors on the static characteristics of the foam, we proposed in this section the best combination of parameters to produce a satisfactory NP-stabilized CO₂ foam under certain geological conditions. Usually, in field practices, the geological temperature, pressure, salinity, and oil presence is already set, we testify

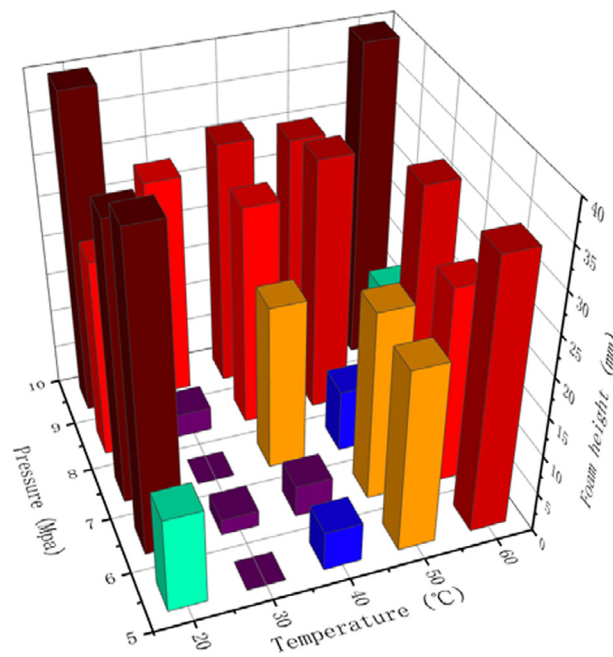


Fig. 16 Synergy effect of temperature and pressure on the foam height results.

therefore the proposed combination of surfactant concentration and NP concentration on the generation of NP-stabilized foam with satisfactory static properties.

Two cases are chosen as an example to show the validity of the multi-parameter screening procedure. The temperature in one case is 45 °C and in another case is 55 °C, in both cases the pressure is 9 MPa, the salinity is 2.5 wt%, and the oil concentration is 2.5 wt%. The set parameters in both cases locate in the studying range but are not the same with any case of the 25 OED experimental sets. Based on the analysis of surfactant

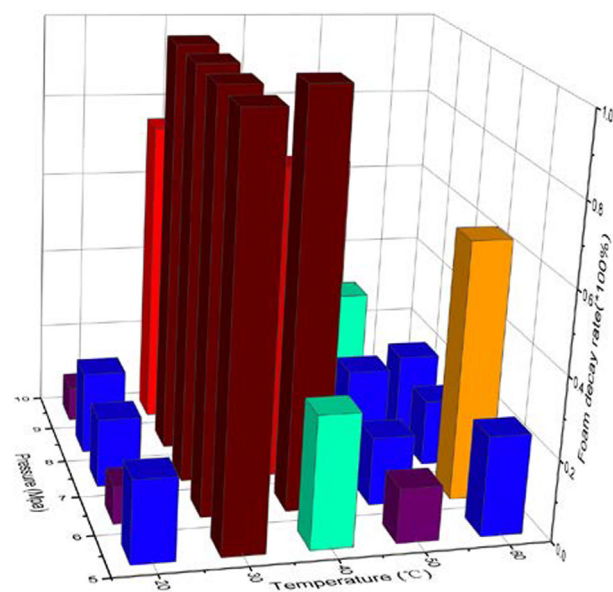


Fig. 17 Synergy effect of temperature and pressure on the foam decay rate results.

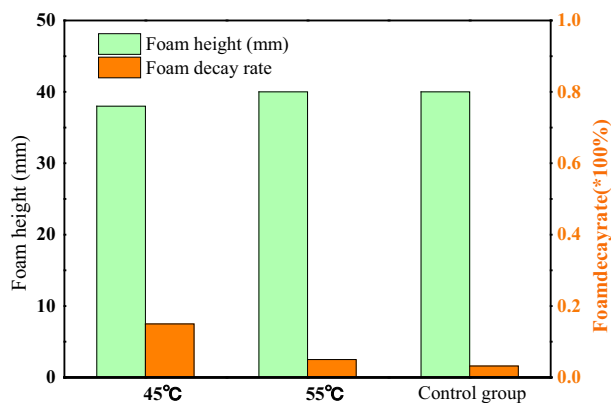


Fig. 18 Foam height and decay rate results under optimal parameter combination (0.4 wt% AOS + 0.15 wt% NP) in comparison with the best results among the 25 studied cases.

and NP concentration effects, as shown in Fig. 8 and Fig. 10 respectively, the best combination of surfactant and NP concentration is determined to be 0.4 wt% and 0.15 wt%.

Fig. 18 displays the foam height and foam decay results obtained with the proposed foam formulation for the two cases, together with the control group results of group 11, which has the best performance on foam static properties among all 25 experiments. It is observed that the proposed parameter combination of surfactant and NP concentration could supply NP-stabilized ScCO₂ foam with satisfactory static properties. The generated foam height could reach 38 mm and 40 mm and the foam decay rates are as low as 0.15 and 0.05 for the cases of 45 °C and 55 °C, behaving satisfactorily in comparison with the best results among all the studied cases. It is concluded, therefore, the proposed optimal composition is efficient and the OED method is feasible to the multi-factor multi-level screening studies of the complex NP-stabilized ScCO₂ foam system for its successful field applications.

4. Conclusions

In this paper, a comprehensive multiple parameter study on the static properties of NP-stabilized CO₂ foam has been carried out. The multi-factor multi-level studies are performed with help of the OED method, and the effects of a single parameter, including surfactant concentration, NP concentration, oil concentration, salinity, temperature, and pressure, as well as synergy effect of temperature and pressure, are thoroughly investigated. Obtained conclusions are listed as follows:

- 1) In the surfactant concentration range of 0.1 wt%~0.5 wt%, the fomability enhances with the increasing surfactant concentration and keeps nearly constant above the concentration of 0.3 wt%, while the foam stability shows continuous improvement with the increasing surfactant concentration.
- 2) In the NP concentration range of 0~0.2 wt%, the increasing NP concentration doesn't lead to obvious foam generation enhancement but results in significant improvement in the foam stability behavior.
- 3) In the oil concentration range of 0 ~ 4 wt%, a higher oil amount doesn't show a significant influence on foamability but results in slightly decreased foam stability.
- 4) In the salinity range of 0 ~ 8 wt%, the effect of salinity on foam generation capacity and foam stability is not obvious.

- 5) Range analysis reveals that The temperature and pressure were the most significant factors for the foam generation capacity, while the temperature is the most significant factors for the foam stability behavior in the temperature range of 20 ~ 60 °C and the pressure range of 5.5 ~ 9.5 MPa. In depth studies on the synergy effect of temperature and pressure reveals that supercritical phase conditions influence significantly the foam static properties. When the system condition is close to the CO₂ critical point, the static properties of the NP-stabilized foam are quite poor, while it behaves much better under conditions that are far from the critical point.
- 6) Optimal formulation of surfactant concentration of 0.4 wt% and NP concentration of 0.15 wt% is proposed for two geological cases of 45 and 55 °C with salinity and oil presence. Good foam static properties are obtained, which verifies the feasibility of the OED method for multiple parameter screening and optimizing studies on the complex NP-stabilized CO₂ foam system.

CRedit authorship contribution statement

Xiakai Song: Investigation, Writing – original draft. **Xincheng Cui:** Formal analysis. **Luming Jiang:** Conceptualization. **Nianhao Ma:** Investigation. **Yong Shu:** Conceptualization. **Jingzhe Li:** Writing – review & editing. **Dongxing Du:** Conceptualization, Methodology, Formal analysis.

Declaration of Competing Interest

The authors declare that they have no known competing financial interests or personal relationships that could have appeared to influence the work reported in this paper.

Acknowledgement

The paper is finished under the supports of the Natural Science Foundation of Shandong Province, China (No. ZR2020ME179) and the research foundation from the Research Institute of Petroleum Exploration and Development of China National Petroleum Company (RIPED-2020-JS-484).

References

- Aarra, M.G., Skauge, A., Solbakken, J., Ormehaug, P.A., 2014. Properties of N₂- and CO₂-foams as a function of pressure. *J. Pet. Sci. Eng.* 116, 72–80.
- Ahadi, A. et al, 2019. Palladium comprising dicationic bipyridinium supported periodic mesoporous organosilica (PMO): Pd@Bipy-PMO as an efficient hybrid catalyst for suzuki-miyaura cross-coupling reaction in water. *Catalysts* 9.
- Akinnikawe, O., Chaudhary, A., Vasquez, O., Enih, C., Ehlig-Economides, C.A., 2010. Increasing CO₂-storage efficiency through a CO₂-brine displacement approach. In: *Soc. Pet. Eng. - SPE Int. Conf. CO₂ Capture, Storage, Util.* 2010, pp. 94–112. <https://doi.org/10.2118/139467-ms>.
- Al Sumaiti, A., Shaik, A.R., Mathew, E.S., Al Ameri, W., 2017. Tuning Foam Parameters for Mobility Control using CO₂ Foam: Field Application to Maximize Oil Recovery from a High Temperature High Salinity Layered Carbonate Reservoir. *Energy Fuels* 31, 4637–4654.
- Alwated, B., El-Amin, M.F., 2021. Enhanced oil recovery by nanoparticles flooding: From numerical modeling improvement to machine learning prediction. *Adv. Geo-Energy Res.* 5, 297–317.

- AlYousef, Z., Almobarky, M., Schechter, D., 2017. Enhancing the Stability of Foam by the Use of Nanoparticles. *Energy Fuels* 31, 10620–10627.
- Antony, J., 2006. Taguchi or classical design of experiments: A perspective from a practitioner. *Sens. Rev.* 26, 227–230.
- Bashir, A., Sharifi Haddad, A., Rafati, R., 2019. Nanoparticle/polymer-enhanced alpha olefin sulfonate solution for foam generation in the presence of oil phase at high temperature conditions. *Colloids Surfaces A Physicochem. Eng. Asp.* 582.
- Beach, R.H. et al, 2019. Combining the effects of increased atmospheric carbon dioxide on protein, iron, and zinc availability and projected climate change on global diets: a modelling study. *Lancet Planet. Heal.* 3, e307–e317.
- Chen, Y. et al, 2014. Switchable Nonionic to Cationic Ethoxylated Amine Surfactants for CO₂ Enhanced Oil Recovery in. *Spe.*
- Dehdari, B., Parsaei, R., Riazi, M., Rezaei, N., Zendejboudi, S., 2020. New insight into foam stability enhancement mechanism, using polyvinyl alcohol (PVA) and nanoparticles. *J. Mol. Liq.* 307, 112755.
- Deng, L., Feng, B., Zhang, Y., 2018. An optimization method for multi-objective and multi-factor designing of a ceramic slurry: Combining orthogonal experimental design with artificial neural networks. *Ceram. Int.* 44, 15918–15923.
- Dhanuka, V.V., Dickson, J.L., Ryoo, W., Johnston, K.P., 2006. High internal phase CO₂-in-water emulsions stabilized with a branched nonionic hydrocarbon surfactant. *J. Colloid Interface Sci.* 298, 406–418.
- Du, D. et al, 2020a. Parameter Screening Study for Optimizing the Static Properties of Nanoparticle-Stabilized CO₂ Foam Based on Orthogonal Experimental Design. *ACS Omega* 5, 4014–4023.
- Du, D. et al, 2020b. Experimental study on rheological properties of nanoparticle-stabilized carbon dioxide foam. *J. Nat. Gas Sci. Eng.* 75, 103140.
- Du, D. et al, 2021. Experimental study on residue oil distribution after the supercritical CO₂ huff-n-puff process in low permeability cores with Nuclear Magnetic Resonance (NMR). *Arab. J. Chem.* 14, 103355.
- Eftekhari, A.A., Krastev, R., Farajzadeh, R., 2015. Foam stabilized by fly-ash nanoparticles for enhancing oil recovery. In: *Soc. Pet. Eng. - SPE Kuwait Oil Gas Show Conf.*. <https://doi.org/10.2118/175382-ms>.
- Emrani, A.S., Nasr-El-Din, H.A., 2015. Stabilizing CO₂-foam using nanoparticles. In: *SPE - Eur. Form. Damage Conf. Proceedings, EFDC 2015-Janua*, pp. 1196–1217.
- Emrani, A.S., Nasr-El-Din, H.A., 2017. An experimental study of nanoparticle-polymer-stabilized CO₂ foam. *Colloids Surfaces A Physicochem. Eng. Asp.* 524, 17–27.
- Emrani, A.S., Ibrahim, A.F., Nasr-El-din, H.A., 2017. Evaluation of mobility control with nanoparticle-stabilized CO₂ foam. In: *SPE Lat. Am. Caribb. Pet. Eng. Conf. Proc.*, pp. 18–19. <https://doi.org/10.2118/185551-ms>.
- Fan, C. et al, 2020. Molecular Dynamics Study on CO₂Foam Films with Sodium Dodecyl Sulfate: Effects of Surfactant Concentration, Temperature, and Pressure on the Interfacial Tension. *Energy Fuels* 34, 8562–8574.
- Farhadi, H., Riahi, S., Ayatollahi, S., Ahmadi, H., 2016. Experimental study of nanoparticle-surfactant-stabilized CO₂ foam: Stability and mobility control. *Chem. Eng. Res. Des.* 111, 449–460.
- Fernø Martin, A. et al, 2016. Experimental study of foam generation, sweep efficiency, and flow in a fracture network. *SPE J.* 21, 1140–1150.
- Fu, C., Liu, N., 2020. Study of the Synergistic Effect of the Nanoparticle-Surfactant-Polymer System on CO₂Foam Apparent Viscosity and Stability at High Pressure and Temperature. *Energy Fuels* 34, 13707–13716.
- Gil-Alana, L.A., Monge, M., 2020. Global CO₂ emissions and global temperatures: Are they related. *Int. J. Climatol.* 40, 6603–6611.
- Guo, F., Aryana, S., 2016. An experimental investigation of nanoparticle-stabilized CO₂ foam used in enhanced oil recovery. *Fuel* 186, 430–442.
- Harati, S., Esfandyari Bayat, A., Sarvestani, M.T., 2020. Assessing the effects of different gas types on stability of SiO₂ nanoparticle foam for enhanced oil recovery purpose. *J. Mol. Liq.* 313, 113521.
- Hosseini-Nasab, S.M., Padalkar, C., Battistutta, E., Zitha, P.L.J., 2016. Mechanistic Modeling of the Alkaline/Surfactant/Polymer Flooding Process under Sub-optimum Salinity Conditions for Enhanced Oil Recovery. *Ind. Eng. Chem. Res.* 55, 6875–6888.
- Hou, P. et al, 2020. Optimize hydrothermal synthesis and electrochemical performance of Li₂FeTiO₄ composite cathode materials by using orthogonal experimental design method. *Ionics (Kiel)*. 26, 1657–1662.
- Jun, S.W. et al, 2013. One-pot synthesis of magnetically recyclable mesoporous silica supported acid–base catalysts for tandem reactions. *Chem. Commun.* 49, 7821–7823.
- Kim, A., Rafiaei, S.M., Abolhosseini, S., Shokouhimehr, M., 2015. Palladium Nanocatalysts Confined in Mesoporous Silica for Heterogeneous Reduction of Nitroaromatics. *Energy Environ. Focus* 4, 18–23.
- Ko, S., Huh, C., 2019. Use of nanoparticles for oil production applications. *J. Pet. Sci. Eng.* 172, 97–114.
- Li, W. et al, 2019. Combined effects of elevated carbon dioxide and temperature on phytoplankton-zooplankton link: A multi-influence of climate change on freshwater planktonic communities. *Sci. Total Environ.* 658, 1175–1185.
- Li, J. et al, 2020. Comparative analysis of different valve timing control methods for single-piston free piston expander-linear generator via an orthogonal experimental design. *Energy* 195, 116966.
- Li, R.F., Hirasaki, G.J., Miller, C.A., Masalmeh, S.K., 2012. Wettability alteration and foam mobility control in a layered, 2D heterogeneous sandpack. *SPE J.* 17, 1207–1220.
- Li, S., Qiao, C., Li, Z., Wanambwa, S., 2017. Properties of Carbon Dioxide Foam Stabilized by Hydrophilic Nanoparticles and Hexadecyltrimethylammonium Bromide. *Energy Fuels* 31, 1478–1488.
- Maestro, A., Rio, E., Drenckhan, W., Langevin, D., Salonen, A., 2014. Foams stabilised by mixtures of nanoparticles and oppositely charged surfactants: Relationship between bubble shrinkage and foam coarsening. *Soft Matter* 10, 6975–6983.
- Majeed, T., Kamal, M.S., Zhou, X., Solling, T., 2021. A Review on Foam Stabilizers for Enhanced Oil Recovery. *Energy Fuels* 35, 5594–5612.
- Osei-Bonsu, K., Shokri, N., Grassia, P., 2015. Foam stability in the presence and absence of hydrocarbons: From bubble- to bulk-scale. *Colloids Surfaces A Physicochem. Eng. Asp.* 481, 514–526.
- Pang, S., Pu, W., Wang, C., 2018. A Comprehensive Comparison on Foam Behavior in the Presence of Light Oil and Heavy Oil. *J. Surfactants Deterg.* 21, 657–665.
- Prigiobbe, V., Worthen, A.J., Johnston, K.P., Huh, C., Bryant, S.L., 2016. Transport of Nanoparticle-Stabilized CO₂Foam in Porous Media. *Transp. Porous Media* 111, 265–285.
- Rezvani, H. et al, 2020. A novel foam formulation by Al₂O₃/SiO₂ nanoparticles for EOR applications: A mechanistic study. *J. Mol. Liq.* 304, 16–18.
- Rognmo, A.U., Horjen, H., Fernø, M.A., 2017. Nanotechnology for improved CO₂ utilization in CCS: Laboratory study of CO₂-foam flow and silica nanoparticle retention in porous media. *Int. J. Greenh. Gas Control* 64, 113–118.
- Rognmo, A.U., Heldal, S., Fernø, M.A., 2018. Silica nanoparticles to stabilize CO₂-foam for improved CO₂ utilization: Enhanced CO₂ storage and oil recovery from mature oil reservoirs. *Fuel* 216, 621–626.
- San, J., Wang, S., Yu, J., Liu, N., Lee, R., 2017. Nanoparticle-stabilized carbon dioxide foam used in enhanced oil recovery: Effect of different ions and temperatures. *SPE J.* 22, 1416–1423.

- Shokouhimehr, M., Asl, M.S., Mazinani, B., 2018. Modulated large-pore mesoporous silica as an efficient base catalyst for the Henry reaction. *Res. Chem. Intermed.* 44, 1617–1626.
- Singh, R., Mohanty, K.K., 2015. Synergy between nanoparticles and surfactants in stabilizing foams for oil recovery. *Energy Fuels* 29.
- Singh, R., Mohanty, K.K., 2020. Study of Nanoparticle-Stabilized Foams in Harsh Reservoir Conditions. *Transp. Porous Media* 131, 135–155.
- Skauge, A., Aarra, M.G., Surguchev, L., Martinsen, H.A., Rasmussen, L., 2002. Foam-Assisted WAG: Experience from the Snorre Field, pp. 1–11, <https://doi.org/10.2118/75157-ms>.
- Song, Z. et al, 2020. A critical review of CO₂ enhanced oil recovery in tight oil reservoirs of North America and China. *Fuel* 276, 118006.
- Telmadarreie, A., Trivedi, J.J., 2020. CO₂ foam and CO₂ polymer enhanced foam for heavy oil recovery and CO₂ storage. *Energies* 13, 1–15.
- Tom-Dery, D., Eller, F., Jensen, K., Reisdorff, C., 2018. Effects of elevated carbon dioxide and climate change on biomass and nutritive value of Kyasuwa (*Cenchrus pedicellatus* Trin.). *J. Appl. Bot. Food Qual.* 91, 88–95.
- Vishal, V., 2017. In-situ disposal of CO₂: Liquid and supercritical CO₂ permeability in coal at multiple down-hole stress conditions. *J. CO₂ Util.* 17, 235–242.
- Wang, Y. et al, 2017. The stability study of CO₂ foams at high pressure and high temperature. *J. Pet. Sci. Eng.* 154, 234–243.
- Wang, Z., Zhang, T., Yu, T., Zhao, J., 2020. Assessment and optimization of grinding process on AISI 1045 steel in terms of green manufacturing using orthogonal experimental design and grey relational analysis. *J. Clean. Prod.* 253, 119896.
- Xiao, C., Balasubramanian, S.N., Clapp, L.W., 2017. Rheology of Viscous CO₂ Foams Stabilized by Nanoparticles under High Pressure. *Ind. Eng. Chem. Res.* 56, 8340–8348.
- Yang, W. et al, 2017a. Foams Stabilized by in Situ-Modified Nanoparticles and Anionic Surfactants for Enhanced Oil Recovery. *Energy Fuels* 31, 4721–4730.
- Yang, W., Wang, T., Fan, Z., 2017b. Highly Stable Foam Stabilized by Alumina Nanoparticles for EOR: Effects of Sodium Cumenesulfonate and Electrolyte Concentrations. *Energy Fuels* 31, 9016–9025.
- Yekeen, N. et al, 2018. A comprehensive review of experimental studies of nanoparticles-stabilized foam for enhanced oil recovery. *J. Pet. Sci. Eng.* 164, 43–74.
- Yu, J., An, C., Mo, D., Liu, N., Lee, R., 2012. Foam mobility control for nanoparticle-stabilized CO₂ foam. *SPE - DOE Improv. Oil Recover. Symp. Proc.* 1, 298–310.
- Yu, J., Khalil, M., Liu, N., Lee, R., 2014. Effect of particle hydrophobicity on CO₂ foam generation and foam flow behavior in porous media. *Fuel* 126, 104–108.
- Zhang, Y. et al, 2015. Dissolution of surfactants in supercritical CO₂ with co-solvents. *Chem. Eng. Res. Des.* 94, 624–631.
- Zhang, P. et al, 2019. Enhanced CO₂ foam based on amide and amine surfactants and synergistically coupled with sodium dodecyl sulfate at high temperature and high pressure. *J. Pet. Sci. Eng.* 179, 266–275.
- Zhang, Q.Y., Qian, J.Q., Guo, H., Yang, S.L., 2008. Supercritical CO₂: A novel environmentally friendly mutagen. *J. Microbiol. Methods* 75, 25–28.
- Zhao, J., Torabi, F., 2020. Experimental investigation and modelling of CO₂-foam flow in heavy oil systems. *Can. J. Chem. Eng.* 98, 147–157.
- Zhu, J., Chew, D.A.S., Lv, S., Wu, W., 2013. Optimization method for building envelope design to minimize carbon emissions of building operational energy consumption using orthogonal experimental design (OED). *Habitat Int.* 37, 148–154.